bioRxiv preprint doi: https://doi.org/10.1101/2022.06.27.497797; this version posted June 27, 2022. The copyright holder for this preprint (which was not certified by peer review) is the author/funder, who has granted bioRxiv a license to display the preprint in perpetuity. It is made available under aCC-BY-NC 4.0 International license.

Extravascular spaces are reservoirs of antigenic diversity in *Trypanosoma brucei* infection

Alexander Beaver[1,2], Nathan P. Crilly[1,2], Jill Hakim[2], Bailin Zhang[2], Bryce Bobb[2], Filipa Rijo-Ferreira[3,4], Luisa Figueiredo[5], and Monica R. Mugnier[2*].

[1] Department of Pathology, Johns Hopkins School of Medicine, Baltimore, Maryland, United States of America

[2] Department of Molecular Microbiology and Immunology, Johns Hopkins Bloomberg School of Public Health, Baltimore, Maryland, United States of America

[3] Department of Neuroscience, Peter O'Donnell Jr. Brain Institute, University of Texas Southwestern Medical Center, Dallas, Texas, United States of America.

[4] Division of Infectious Diseases and Vaccinology, Berkeley Public Health Molecular and Cell Biology Department, Berkeley, California, United States of America

[5] Instituto de Medicina Molecular, Faculdade de Medicina, Universidade de Lisboa, Lisboa, Portugal

* Corresponding author
E-mail: mmugnie1@jhu.edu (MRM)

Abstract

Trypanosoma brucei lives an entirely extracellular life cycle in its mammalian host, facing a constant onslaught of host antibodies. The parasite evades clearance by the host immune system through antigenic variation of its dense variant surface glycoprotein (VSG) coat, periodically "switching" expression of the VSG using a large genomic repertoire of VSG-encoding genes. Studies of antigenic variation *in vivo* have focused exclusively on parasites in the bloodstream, but recent work has shown that many, if not most, parasites are extravascular and reside in the interstitial spaces of tissues. However, it is unknown whether parasites undergo antigenic variation while in extravascular spaces. We sought to explore the dynamics of antigenic variation in extravascular parasite populations using VSG-seq, a high-throughput sequencing approach for profiling VSGs expressed in populations of *T. brucei*. Our experiments show that the expressed VSG repertoire is not uniform across populations of parasites within the same infection and that a greater number of VSGs are expressed in tissue spaces than in the blood. More than 75% of the VSGs detected in an animal were found exclusively within extravascular spaces. Interestingly, we also noticed a delay in the VSG-specific clearance of parasites in tissue spaces compared to the blood. This finding aligns with a model in which parasites "hide" from the immune system in tissue spaces, where a slower immune response provides them with more time to generate new antigenic variants. Overall, our results show that extravascular spaces are significant reservoirs of VSG diversity, potentially resulting from delayed clearance of tissue-resident parasites.

bioRxiv preprint doi: https://doi.org/10.1101/2022.06.27.497797; this version posted June 27, 2022. The copyright holder for this preprint (which was not certified by peer review) is the author/funder, who has granted bioRxiv a license to display the preprint in perpetuity. It is made available under aCC-BY-NC 4.0 International license.

Introduction

Trypanosoma brucei is a eukaryotic unicellular parasite and the causative agent of human and animal African Trypanosomiasis[1]. Transmitted by the bite of the tsetse fly, it lives extracellularly in the hosts' blood, lymphatic system, interstitial tissue spaces, and central nervous system[2,3]. Human African trypanosomiasis, a neglected tropical disease, is typically fatal if left untreated. Illness in domestic animals, which can also serve as large parasite reservoirs, results in a significant economic burden to rural Africa[4,5].

T. brucei parasites live an entirely extracellular life cycle and face continuous exposure to the host's immune system during infection. To deal with this onslaught of host antibodies, the parasite has evolved a sophisticated mechanism of antigenic variation. *T. brucei* is surrounded by a dense coat of variant surface glycoprotein (VSG). ~10^7 copies of a single VSG pack onto the parasite's plasma membrane, shielding invariant membrane proteins from immune detection. Though VSG is easily detected by the host immune system[6], *T. brucei* periodically "switches" expression of the VSG on its surface, using a genomic repertoire of ~2800 different VSG-encoding genes and pseudogenes[7–10]. Parasites expressing these new VSGs are able to avoid immune clearance. In addition to drawing from its large genomic VSG repertoire, *T. brucei* can create novel VSGs using homologous recombination between two or more VSG genes or pseudogenes[11,12]. These mechanisms give *T. brucei* an enormous capacity for altering its antigenic profile. This arms race between parasites and the host immune system generates waves of parasitemia that are characteristic of *T. brucei* infections[13].

Studies examining *T. brucei* antigenic variation *in vivo* have revealed complex dynamics in which populations of parasites express many different VSGs at both peaks and valleys of parasitemia. Indeed, VSG diversity in the blood is much higher than was initially suspected to be required for immune evasion[14–16]. It has recently become clear, however, that extravascular spaces represent an important niche for *T. brucei*, in both experimental and natural infections[17,18]. Within a week post-infection, tissue-resident parasites make up the majority of parasites in a mouse infection[19], and significant reservoirs of parasites have been found in the interstitial areas of nearly every organ[20,21]. In addition, *T. brucei* parasites within the adipose, skin, and brain have altered gene expression profiles, suggesting an adaption to their tissue environment[20,22,23]. Extravascular parasites have also been shown to be associated with increased disease severity[19]. While it is clear parasites adapt to extravascular spaces, the precise role of tissue-resident parasites in infection remains unclear, and their contribution to antigenic variation has not been studied.

Interestingly, parasite tissue tropisms related to antigenic variation have been reported in other organisms. For example in *Plasmodium Falciparum,* expression of a single *var* gene, *var2csa*, allows for parasites to be sequestered in the placenta, aiding in immune evasion and causing severe placental malaria[24,25]. Similarly, the pili *of Neisseria gonorrhoeae* have critical functions in both antigenic variation and adhesion to host tissue[26]. In some cases, specific *T. brucei* VSG genes have gained functions besides antigenic variation[27,28] and VSGs have been shown to potentially influence parasite growth[29]. It is thus plausible that similar VSG-dependent tropisms exist in *T. brucei* infections, either influencing tissue invasion or adaptation to tissue spaces.

In this study, we sought to evaluate the role of extravascular parasites in antigenic variation during *T. brucei* infection. We found that blood and tissue-resident parasites express distinct VSG repertoires, even within the same infected mouse, showing that parasite populations in the blood do not fully represent the antigenic complexity of *T. brucei* populations *in vivo*. Moreover, tissue-resident parasites account for most of the antigenic diversity in an infection, serving as a

bioRxiv preprint doi: https://doi.org/10.1101/2022.06.27.497797; this version posted June 27, 2022. The copyright holder for this preprint (which was not certified by peer review) is the author/funder, who has granted bioRxiv a license to display the preprint in perpetuity. It is made available under aCC-BY-NC 4.0 International license.

reservoir of new VSGs with the potential to contribute to immune evasion. We also observed a delay in VSG-specific parasite clearance in tissue spaces compared to the blood which could explain the elevated VSG diversity observed in these spaces. Overall, our results demonstrate that tissue-resident *T. brucei* parasites play a distinct role in immune evasion during infection, highlighting the intimate interplay between antigenic variation and the host environment.

bioRxiv preprint doi: https://doi.org/10.1101/2022.06.27.497797; this version posted June 27, 2022. The copyright holder for this preprint (which was not certified by peer review) is the author/funder, who has granted bioRxiv a license to display the preprint in perpetuity. It is made available under aCC-BY-NC 4.0 International license.

Results

VSG diversification occurs after tissue invasion

To investigate the expressed VSG repertoire of *T. brucei* parasites within the blood and tissues of infected mice, we intravenously injected 12 mice with ~5 pleomorphic *T. brucei* EATRO1125 AnTat1.1E 90-13 parasites[30]. We tracked parasitemia in the blood throughout infection (Figure 1A) and collected the heart, lungs, gonadal fat, subcutaneous fat, brain, and skin at each of three time points: days 6, 10, and 14. For each mouse, blood was collected on days 6, 10, and 14 or until the mouse was sacrificed for tissue collection. Because tissue collection is terminal, each time point is represented by a distinct set of 4 mice. For each sample, we extracted RNA and quantified VSG expression using VSG-Seq. To compare VSG expression between samples, we grouped VSG open reading frames (ORFs) with >98% identity into VSG "clusters." We then used qPCR to estimate parasite load in each tissue sample and filtered out VSGs that represented less than one parasite (Figure 1B). The number of VSGs in a sample did not correlate with either the number of reads aligned or the number of parasites in a sample (Supplemental Figure 1A & B), suggesting that sampling of each population was sufficient. In total, we identified 1,074 distinct VSGs in all infected mice.

Our analysis of VSG expression in the blood and tissues revealed that initial populations are quite similar with respect to VSG expression. Because a small inoculum was used, each of these infections was essentially clonal, with a single VSG (either AnTat1.1 or EATRO1125 VSG-421) dominating expression in the blood on day 6 post-infection. This "initiating VSG" was also the major population in every tissue space on day 6 (Figure 1C). This early uniformity in VSG expression suggests that in this model of infection *T. brucei* invades tissues before significant VSG switching has occurred.

bioRxiv preprint doi: https://doi.org/10.1101/2022.06.27.497797; this version posted June 27, 2022. The copyright holder for this preprint (which was not certified by peer review) is the author/funder, who has granted bioRxiv a license to display the preprint in perpetuity. It is made available under aCC-BY-NC 4.0 International license.

133
134

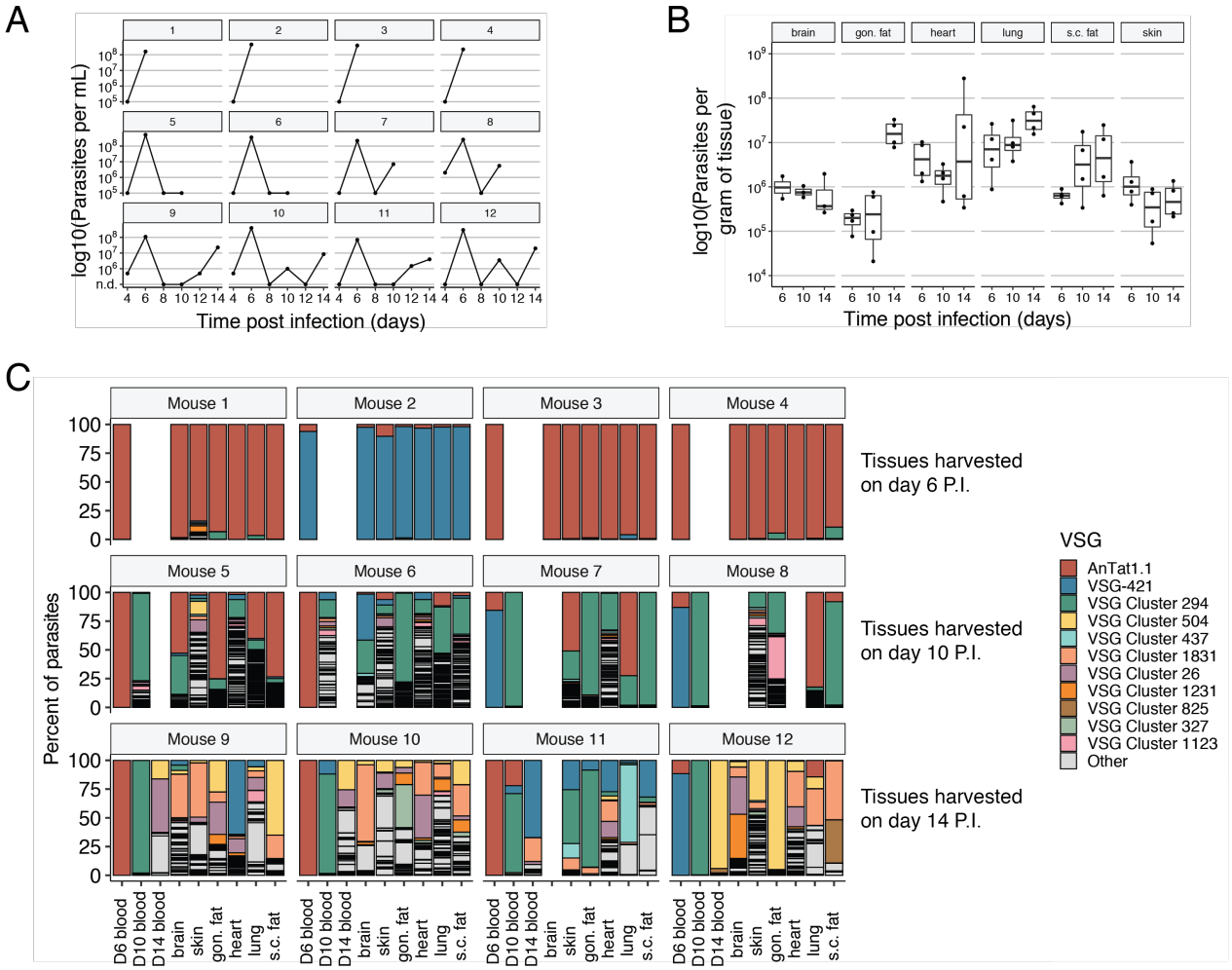

Figure 1: Extravascular populations diversify independently *in vivo*. (A) Parasitemia of 12 mice infected with AnTat1.1E *T. brucei* counted from tail blood by hemocytometer (n.d. = not detectable). **(B)** Estimated parasite load per gram from QPCR performed on RNA extracted from perfused and homogenized tissue samples (s.c. fat = subcutaneous fat; gon. fat = gonadal fat). **(C)** The percent of parasites expressing each VSG within a space. The top 11 VSGs with the highest overall expression are colored and all other VSGs are in grey as “other”. Each row, from the top down, represents mice that were harvested on day 6, 10, and 14, respectively. Day 10 and day 14 mice also have matching blood samples from earlier time points.

bioRxiv preprint doi: https://doi.org/10.1101/2022.06.27.497797; this version posted June 27, 2022. The copyright holder for this preprint (which was not certified by peer review) is the author/funder, who has granted bioRxiv a license to display the preprint in perpetuity. It is made available under aCC-BY-NC 4.0 International license.

VSG clearance is delayed in tissues compared to the blood

Because parasite populations in all spaces on day 6 were so similar, we were able to track the clearance of parasites expressing the initiating VSG in blood and tissue spaces. Parasites expressing the initiating VSG were undetectable in every blood sample on day 10 post-infection but remained detectable in 23/24 (~96%) tissue samples. Despite its absence in the blood, the initiating VSG still represented a majority of parasites in some tissue spaces on day 10. By day 14, however, parasites expressing the initiating VSG were undetectable in most spaces (Figure 2A). Notably, there was no correlation between any specific tissue and the proportion of the population still expressing the initiating VSG.

To confirm this result from the VSG sequencing data, we performed flow cytometry on parasites from the blood and tissues of mice infected with a tdTomato-expressing “triple reporter” *T. brucei* EATRO1125 AnTat 1.1E cell line[31]. These parasites express tdTomato in their cytoplasm and then we stained samples with an anti-AnTat1.1 antibody. We found that in the blood on day 13 on average 0.02% of parasites, just above our limit of detection for VSG-seq, expressed AnTat1.1, while on average 1.73% of parasites within the lungs and gonadal fat stained positive for AnTat1.1 (Figure 2B and 2C). These data corroborate measurements by VSG-seq and show that parasites expressing AnTat1.1 persist within tissues after they have been cleared from the blood. As parasites appear to eventually be cleared from tissue spaces, these results are consistent with a model in which the clearance of parasites within extravascular spaces is delayed, but not abolished, compared to the blood.

bioRxiv preprint doi: https://doi.org/10.1101/2022.06.27.497797; this version posted June 27, 2022. The copyright holder for this preprint (which was not certified by peer review) is the author/funder, who has granted bioRxiv a license to display the preprint in perpetuity. It is made available under aCC-BY-NC 4.0 International license.

158

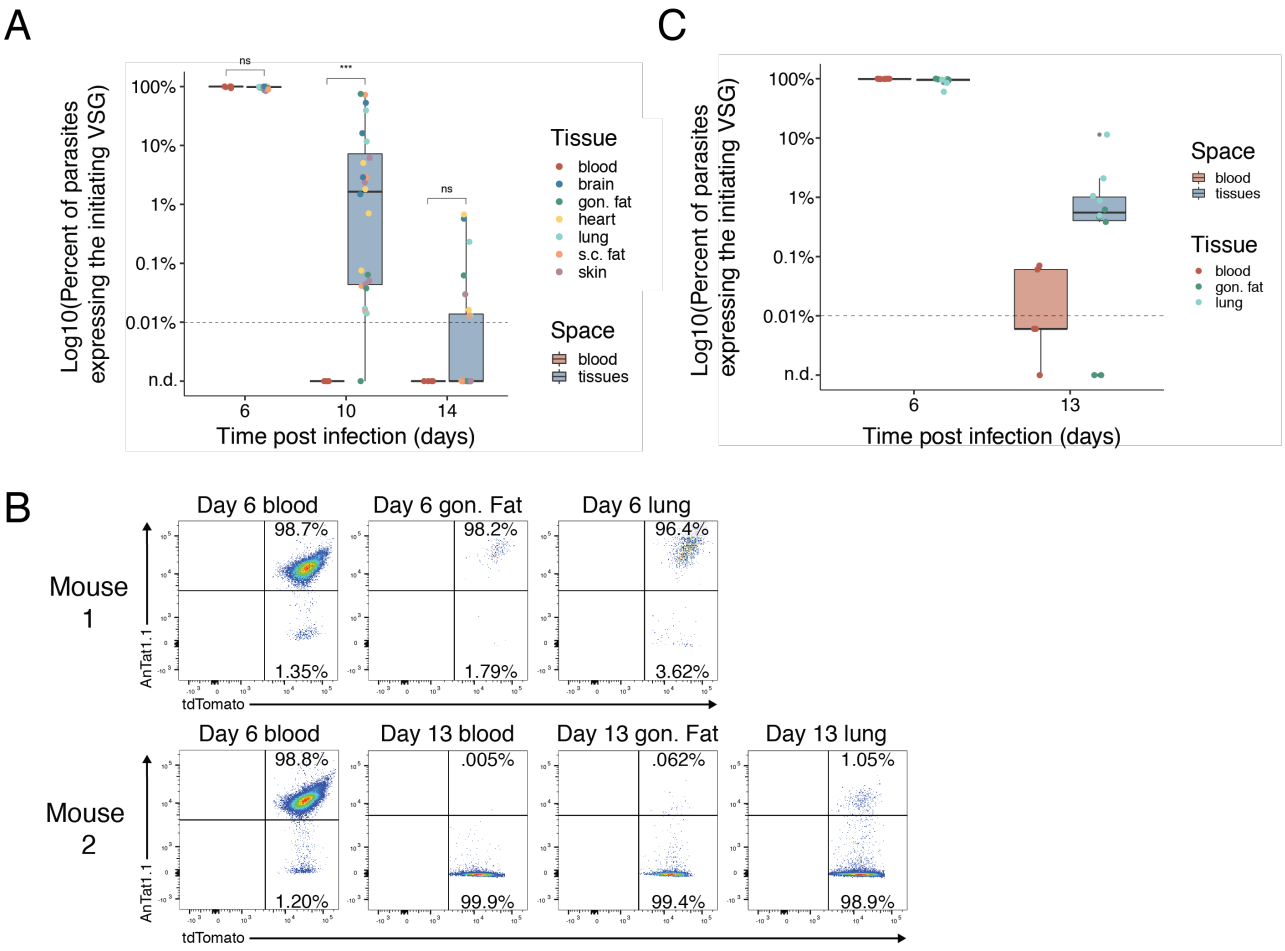

Figure 2: Clearance of parasites expressing the initiating VSG is delayed in tissues compared to the blood. (A) The percent of parasites (log10) expressing the infection initiating VSG (AnTat1.1 or VSG-421) at each time point. Tissue samples were grouped together (blue) and compared to blood samples (red). Statistical significance was determined by a pairwise Wilcoxon test. The horizontal dotted line represents the VSG-seq limit of detection. **(B)** Representative flow cytometry plots from tissues collected from mice infected with chimeric triple marker parasites that express tdTomato constitutively in their cytoplasm. Parasites were stained with anti-AnTat1.1 antibody. The top row shows blood and tissues from one mouse that was collected on day 6 P.I. and the second row shows blood collected from a mouse on both day 6 and day 13 and tissues from day 13 P.I. **(C)** Quantification of the number of parasites that were tdTomato positive and stained positive for AnTat1.1 by flow cytometry (n = 5 per group). The horizontal dotted line marks the limit of detection of VSG-seq.

bioRxiv preprint doi: https://doi.org/10.1101/2022.06.27.497797; this version posted June 27, 2022. The copyright holder for this preprint (which was not certified by peer review) is the author/funder, who has granted bioRxiv a license to display the preprint in perpetuity. It is made available under aCC-BY-NC 4.0 International license.

VSG diversification is not uniform across spaces within a mouse

Host humoral immunity and antigenic variation are intrinsically intertwined. As parasites expressing specific VSGs are cleared, other switched parasites persist. We see that as infection progresses and the initiating VSG disappears, VSG expression in populations begins to diverge. On days 10 and 14, the VSG composition of each space is different, and no single VSG dominates. Importantly, VSG expression in the blood no longer matches expression in tissue spaces (Figure 1C). However, we still often see the same VSGs expressed within populations, both within and between infected mice, although in varying compositions. On days 10 and 14, the top eleven most highly expressed VSGs represent an average of 84.07 % and 67.55%, respectively, of parasites in every space. This suggests that the semi-predictable switching hierarchy previously observed within the blood governs antigenic variation in tissue spaces[14,32].

Tissue-resident parasites account for most of the antigenic diversity in infections

The stochasticity of *T. brucei's* semi-predictable switching hierarchy, however, allows tissue-resident populations to diverge from the blood and from one another. In addition to this frequently expressed subset, populations display a huge diversity of VSGs. At any time, most of the antigenic diversity in an infection is found exclusively within extravascular spaces. In each mouse, 77.19%-94.0% of expressed VSGs were detected exclusively in tissues, while only 0.41% to 5.0% of VSGs are found exclusively within the blood (Figure 3A and 3B). Individual tissue spaces generally harbor more VSGs than the blood as well (Figure 3C). Given the large number of VSGs unique to these spaces, we sought to address whether certain VSGs were more likely to emerge in certain tissue microenvironments. Notably, we found no evidence for tissue-specific VSGs or VSG sequence motifs (Supplemental Figure 2).

Central to antigenic variation is the expression of new VSGs to which the host immune system has not yet been exposed. To evaluate the potential for tissue-resident parasite populations to generate new variants, and thus facilitate immune evasion, we examined the proportion of VSGs expressed in each space that are only found within that space in a mouse. We termed these "unique" VSGs (Figure 4A). Day 6 samples were excluded from this analysis because very few VSGs are expressed at this time point. Between 4.8% to 35.5% of VSGs within any space are unique to that space. Tissue spaces generally display a greater proportion of unique VSGs than the blood (Figure 4B), though these unique VSGs typically represent a relatively small proportion of the total parasite population in each space (Figure 4C). Taken together these results suggest that tissue-resident populations are diversifying independently and that blood-resident parasites alone do not reflect the complexity of antigenic variation *in vivo*. There is the potential capacity for parasites in every space to contribute new antigenic variants to an infection.

bioRxiv preprint doi: https://doi.org/10.1101/2022.06.27.497797; this version posted June 27, 2022. The copyright holder for this preprint (which was not certified by peer review) is the author/funder, who has granted bioRxiv a license to display the preprint in perpetuity. It is made available under aCC-BY-NC 4.0 International license.

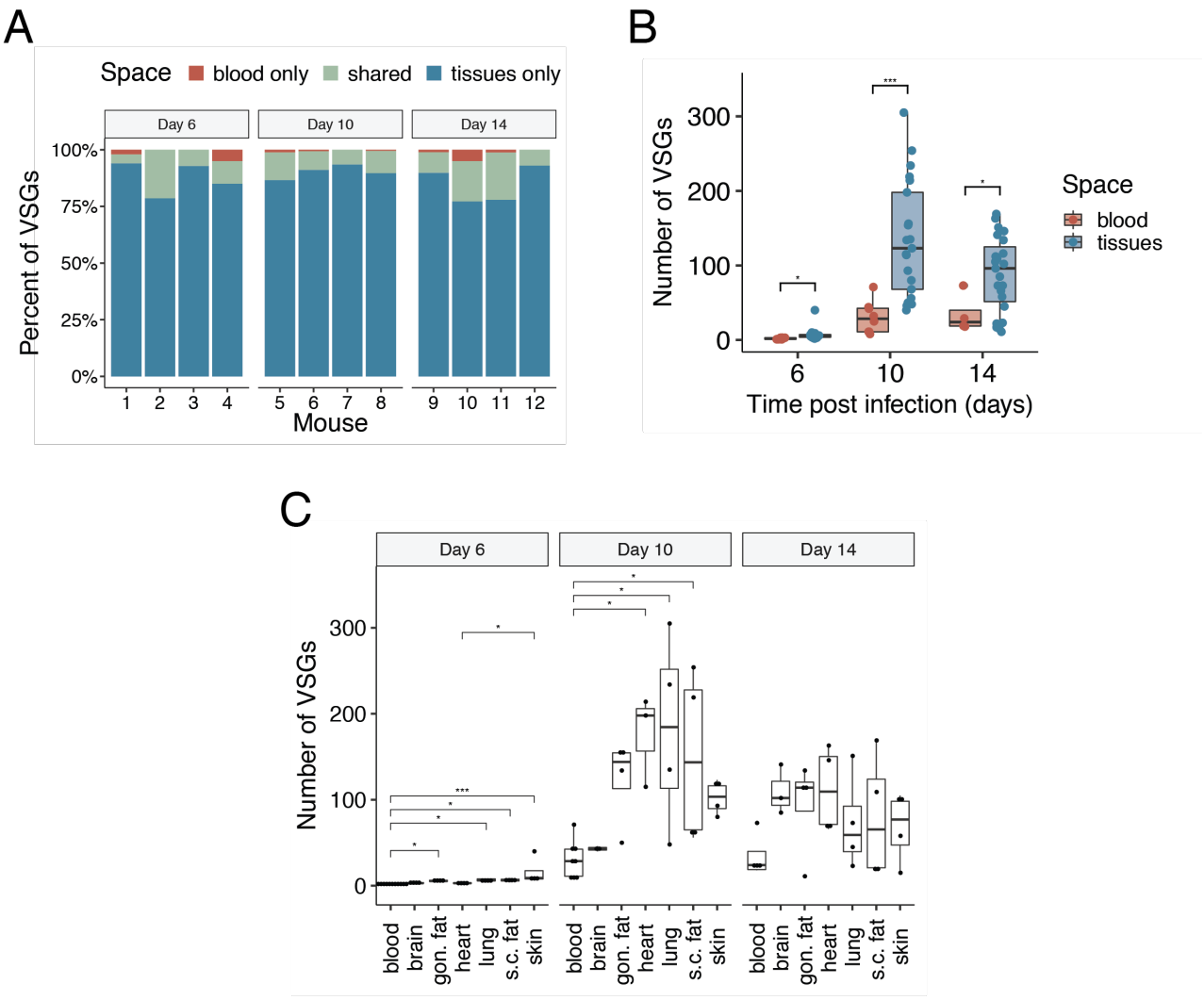

Figure 3: Populations of extravascular parasites harbor most of the antigenic diversity in an infection. (A) Stacked bar graphs from each mouse representing the proportion of VSGs that were found exclusively within the blood (red), exclusively within tissue spaces (blue), or shared by both the blood and at least one tissue space (green). **(B)** Quantification of the number of VSGs found within the blood (red) or tissue spaces (blue) at each timepoint. Each point represents a blood or tissue sample from a mouse. Statistical significance was determined by a Student's t-test between the blood and tissues within each timepoint. **(C)** The number of VSGs represented in each tissue space (for each tissue and day 14 blood; n= 4, for day 6 blood n = 12, for day 10 blood n =8). A pairwise Dunnett's test was performed between all spaces within each timepoint.

bioRxiv preprint doi: https://doi.org/10.1101/2022.06.27.497797; this version posted June 27, 2022. The copyright holder for this preprint (which was not certified by peer review) is the author/funder, who has granted bioRxiv a license to display the preprint in perpetuity. It is made available under aCC-BY-NC 4.0 International license.

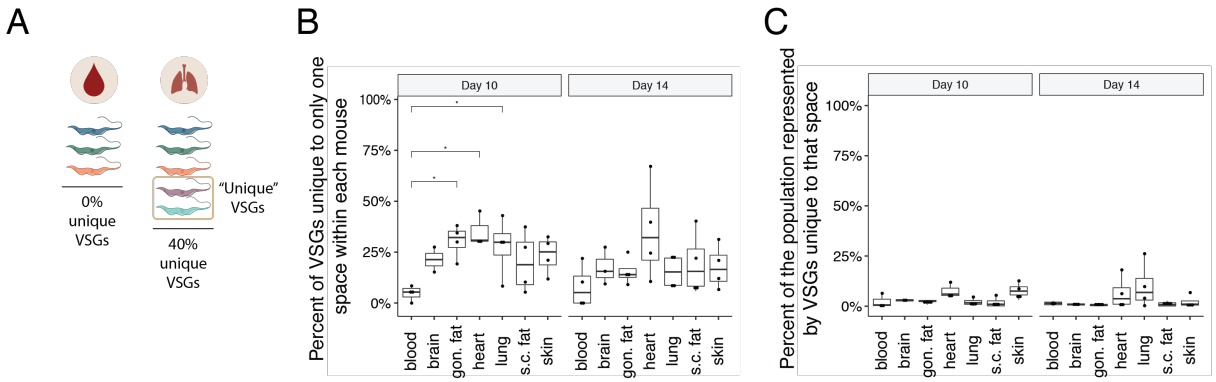

Figure 4: Tissue-resident parasites have the potential to contribute unique VSGs to an infection. (A) We define "unique" VSGs as those VSGs solely found within a specific space in a mouse (Created with BioRender.com). **(B)** The percent of VSGs that were unique to one space within a mouse (n = 4 per group). Statistical significance was determined using a pairwise Dunnett's test. **(C)** The percentage of each population represented by unique VSGs.

VSGs initially only seen in tissues can be found in all spaces later during infection

Tissue spaces harbor many VSGs unique to the extravascular niche, but many of these are expressed by a small number of parasites. We sought to understand whether these rare VSGs exclusive to tissues had the potential to establish within other spaces in the host, suggesting a role in immune evasion, or if they simply represented dead ends for the parasite. To address this question, we identified VSGs only expressed in tissues on day 6 post-infection and analyzed their fates at later timepoints, specifically looking to see if they appeared later within the blood. Of these 58 VSGs only in tissues on day 6, 43 (74.1%) were expressed on day 10 or day 14 within the blood. By examining a few of these VSGs more closely, we saw that VSG cluster 294, which was initially only expressed in tissues on day 6, represented a large proportion of parasites on day 10, particularly within the blood. Interestingly, we also observed the same delayed clearance of VSG cluster 294 within extravascular spaces as we had previously seen with the initiating VSG. VSG clusters 504 and 1831 also represented small populations of parasites in tissues on day 6, but later become highly expressed in both the blood and tissue spaces (Figure 5). Thus, rare VSGs expressed at low levels exclusively in tissue spaces have the potential to become ubiquitously expressed within a host, raising interesting questions about the ability for tissue parasites to reseed the blood, aiding in immune evasion.

bioRxiv preprint doi: https://doi.org/10.1101/2022.06.27.497797; this version posted June 27, 2022. The copyright holder for this preprint (which was not certified by peer review) is the author/funder, who has granted bioRxiv a license to display the preprint in perpetuity. It is made available under aCC-BY-NC 4.0 International license.

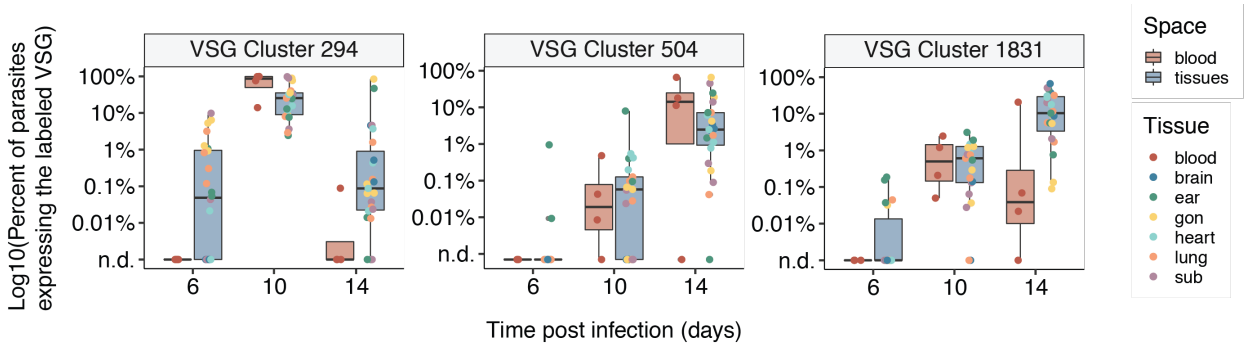

Figure 5: VSGs only seen in tissues on day 6 are often seen in the blood and tissues later during infections. The expression (log10) of VSG cluster 294, 504, and 1831 within all samples on days 6, 10, and 14. Samples were grouped into two groups, blood (red) or tissues (blue).

Discussion

Previous *in vivo* studies of antigenic variation in *T. brucei* have investigated the phenomenon solely in blood-resident parasite populations[12,14,15]. Recent work, however, has revealed that large numbers of parasites reside in extravascular spaces outside of the bloodstream[3,17,20]. Here we show that the majority of the antigenic diversity during infection is found exclusively within these tissue-resident populations of *T. brucei* parasites. Moreover, individual extravascular parasite populations often express more VSGs than populations in the blood. VSGs detected at low levels in tissues at early time points post-infection can become highly expressed VSGs within the blood at later time points, suggesting these extravascular reservoirs of antigenic diversity could be vital for parasite immune evasion and disease chronicity.

The renewed interest in tissue-resident *T. brucei* parasites has generated speculation about the possibility that VSGs could play a role in tissue tropism for *T. brucei*. Interestingly, we saw no evidence of tissue-specific VSG expression in these experiments. Because parasites invade tissues efficiently before significant VSG switching has occurred, it appears unlikely that any specific VSG is required for tissue invasion. Whether some VSGs may provide an adaptation to specific host spaces is less clear. We only measured VSG expression up to day 14 post-infection, at which point tissue-resident populations were just beginning to diverge from one another and the blood. It is therefore possible that, as these populations further evolve, there may be selection for VSGs better adapted to certain tissue spaces. It is also possible that a relationship between VSG expression and tissue tropism could emerge in an infection initiated by a tsetse bite, where the inoculum is larger[36] and likely more antigenically diverse.

Instead of tissue-specific VSG expression, our data support a model in which each tissue-resident population is evolving independently, influenced by the same semi-predictable switching hierarchy that has been seen to govern VSG expression in the blood[14,37]. Nevertheless, the scale of antigenic variation in these spaces is quite different. The number of VSGs we detected in the blood corroborates previous estimates[12,14,15], but the diversity in tissue spaces is, on average, two to four times higher than the blood. Overall, tissue-resident populations harbor ~95% of the antigenic diversity in any given infection.

It is unclear what mechanisms or circumstances lead to the increased diversity we observe in extravascular spaces. Why do tissue spaces harbor so many more VSGs? One intriguing possibility is that parasites in tissue spaces are actually switching at a higher rate than those in

bioRxiv preprint doi: https://doi.org/10.1101/2022.06.27.497797; this version posted June 27, 2022. The copyright holder for this preprint (which was not certified by peer review) is the author/funder, who has granted bioRxiv a license to display the preprint in perpetuity. It is made available under aCC-BY-NC 4.0 International license.

the blood. The mechanisms that initiate VSG switching during infection remain poorly understood. While DNA double-strand breaks can trigger VSG switching *in vitro*[38,39], it remains unclear whether they serve as a natural trigger for switching *in vivo*. It is plausible to speculate that some aspect of the extravascular environment could supply a molecular or physical stimulus that promotes VSG switching, leading to increased VSG diversity within these spaces.

A second, and not mutually exclusive, explanation for the increased antigenic diversity in tissue spaces lies in the observation that VSG-specific clearance of parasites is delayed in extravascular spaces. By day 10 post-infection, parasites expressing the initiating VSG are undetectable in the blood but remain in tissue spaces until at least day 14. Perhaps parasites within these spaces, which survive longer before being cleared, simply have more opportunity to switch. An increased survival time would allow extravascular populations to accumulate many more switched parasites over time, resulting in the higher VSG diversity we observe. Thus, extravascular spaces could serve as a haven for diversification and a reservoir of antigenic diversity to seed the blood.

This increased diversity could be vital in natural infections, particularly in wild animals, where pre-existing anti-VSG immunity is more likely to exist. In this case, a high rate of switching may be required to successfully evade the host's existing anti-VSG antibody repertoire. For extravascular populations to impact systemic antigenic variation, however, extravascular parasites must be able to exit tissue spaces and enter the blood. Vascular permeability is high after the initial stages of infection[19], suggesting parasites likely move back and forth between spaces, but this has not yet been definitively demonstrated. It will thus be critical to demonstrate that parasites can move from tissue spaces to the blood. Nevertheless, our data are consistent with a model in which variants generated in tissues later seed the blood: rare variants detected exclusively within tissue spaces on day 6 post-infection can be detected at high levels in the blood at later timepoints.

While the immune response in extravascular spaces is clearly distinct from the blood, the nature of the immune response in these spaces that leads to a delay in VSG-specific parasite clearance is unknown. Perhaps surprisingly, our data suggest the mechanism is not organ-specific. Instead, delayed clearance and increased antigenic diversity appear to be general features of extravascular infection. This fact points to one possible explanation for the delay we observe. IgM, a bulky pentamer, is the first antibody to respond to infection and initiates around day 6 with a peak around day 10 post-infection in mice. IgG, on the other hand, is a monomer that peaks around day 14 post-infection[40,41]. There is some evidence that IgM cannot diffuse into tissue spaces adequately[42,43]. If anti-VSG IgM diffuses poorly into extravascular spaces, then extravascular parasites would not be fully cleared until IgG is produced. We observe clearance in extravascular spaces that coincides with peak serum levels of IgG, supporting this model. Of course, it is also possible that local extravascular immune responses mount with different dynamics than the systemic response. Whatever the mechanism, it is apparent that extravascular spaces are distinct from the blood in multiple ways.

Our experiments demonstrate that extravascular spaces serve as important reservoirs of VSG during *T. brucei* infection, accounting for the vast majority of antigenic diversity in any individual infection. Our data suggest that this could be due, in part, to a delayed immune response in extravascular spaces that allows parasites to survive longer and switch more. This study raises compelling questions about the nature of extravascular immunity, initiation of VSG switching *in vivo,* and the process of reseeding parasites into the blood. Overall, our results establish extravascular spaces as an important and previously overlooked niche for antigenic variation in *T. brucei.*

bioRxiv preprint doi: https://doi.org/10.1101/2022.06.27.497797; this version posted June 27, 2022. The copyright holder for this preprint (which was not certified by peer review) is the author/funder, who has granted bioRxiv a license to display the preprint in perpetuity. It is made available under aCC-BY-NC 4.0 International license.

Methods

Mouse infections and sample collection

12 female C57Bl/6J (Jackson Laboratory) between 7-10 weeks old were each infected by intravenous tail vein injection with ~5 pleiomorphic EATRO 1125 AnTat1.1E 90-13 *T. brucei* parasites[30]. Blood parasitemia was counted by tail bleed every 2 days starting on day 4 post-infection (PI) by hemocytometer. Blood (25uL) was collected by a submandibular bleed on days 6, 10, and 14 PI and placed into TRIzol LS. Four Mice were anesthetized and perfused at each time point (days 6, 10, and 14 PI). Mice were perfused with 50mL of PBS-Glucose (0.055M D-glucose) with heparin. After perfusion, tissues were dissected and placed immediately into 1mL of RNA later. The heart, lungs, gonadal fat, subcutaneous fat, brain, and skin (ear) were collected.

For flow cytometry experiments, 7-10 week old female C57Bl/6J mice were infected by intravenous tail vein injection with ~5 AnTat1.1E chimeric triple reporter *T. brucei* parasites which express tdTomato[31]. Blood was collected by a submandibular bleed at each time point. Mice were anesthetized and perfused on days 6 and 13 P.I. as discussed above and the gonadal fat and lungs were harvested.

VSG-seq sample and library preparation

RNA was isolated from blood samples stored in TRIzol LS (ThermoFisher, 10296010) by phenol/chloroform extraction. Tissue samples were weighed and homogenized in TRIzol, and then RNA was isolated by phenol/chloroform extraction. RNA from each sample was DNase treated using Turbo DNase and cleaned up with Mag-Bind® TotalPure NGS beads (Omega Bio-Tek M1378-00). First-strand cDNA synthesis was performed using SuperScript III Reverse Transcriptase and a primer that binds to the conserved VSG 14-mer in the 3´-UTR (5'-GTGTTAAAATATATC-3'). Products were cleaned up using Mag-Bind® TotalPure NGS beads (Omega Bio-Tek, M1378-01). Next, a VSG-specific PCR with Phusion polymerase (ThermoFisher, F530L) was performed using primers for the spliced leader (5'-ACAGTTTCTGTACTATATTG-3') and SP6-VSG 14-mer sequences (5'-GATTTAGGTGACACTATAGTGTTAAAATATATC-3') for 25 cycles. VSG-PCR products were cleaned up using Mag-Bind® TotalPure NGS beads and quantified using the QuBit HS DNA kit (Life Technologies). Finally, sequencing libraries were prepared with the Nextera XT DNA Sample Prep Kit (Illumina) using the manufacturer's guidelines, and libraries were sequenced with 100bp single-end reads on an Illumina HiSeq 2500.

Tissue QPCR

First-strand synthesis was performed with SuperScript III Reverse Transcriptase (Thermo Fisher Scientific, 18080051) and random hexamers primers on tissue RNA samples. QPCR was performed in triplicate using SYBR Green qPCR Master Mix (Invitrogen, 4309155). ZFP3 primers were used to estimate parasite load in tissue samples (FW: 5'-CAGGGGAAACGCAAAACTAA-3'; RV: 5'-TGTCACCCCAACTGCATTCT-3'). CT values were averaged between the triplicates and parasite load per mg of tissue were estimated using a standard curve of values from RNA isolated from known numbers of cultured parasites.

bioRxiv preprint doi: https://doi.org/10.1101/2022.06.27.497797; this version posted June 27, 2022. The copyright holder for this preprint (which was not certified by peer review) is the author/funder, who has granted bioRxiv a license to display the preprint in perpetuity. It is made available under aCC-BY-NC 4.0 International license.

VSG-seq analysis

Analysis of sequencing results was performed following the method we reported previously[14], with two changes: no mismatches were allowed for bowtie alignments and each sample was analyzed (assembly, alignment, and quantification) separately. To compare expressed VSG sets between samples, all assembled VSGs were clustered using CD-HIT-EST[44], with VSGs with >98% identity grouped into clusters. VSGs were then identified by their Cluster number for further analysis. Samples that had less than 100,000 successfully aligning reads to VSGs were excluded from further analysis. Four samples, 3 brain and 1 heart, were discarded because fewer than 100,000 reads aligned to VSG (Supplemental Figure 1A). Downstream analysis of expression data and generation of figures was performed in R. Code for generating the analysis and figures in this paper are available at https://github.com/mugnierlab/Beaver2022.

Analysis of VSG sequence motifs

To identify tissue-specific VSGs, the similarity of N terminal sequences from all assembled VSGs were compared. N terminal sequences were identified using a HMMER scan against a database curated by Cross et al. Then all N termini were compared in an all vs all blast using default parameters. All VSG pairwise comparisons with an e-value higher than 1E-3 were considered sufficiently similar to one another for further analysis. VSGs that were found in a given tissue were binned into that tissue group, and the distribution of the bitscores in a given compartment was compared against the total population of similar VSGs.

Flow Cytometry

Once mice were perfused, tissues were dissected and washed with HBSS (Hanks balanced salt solution, ThermoFisher Scientific 14175095). Tissue samples were minced and placed in DMEM (ThermoFisher Scientific, 11995065) containing either 1 mg/mL collagenase type 1 (ThermoFisher Scientific, 17100017) for adipose fat or 2 mg/mL collagenase type 2 (ThermoFisher Scientific, 17101015) for lung samples. These were then incubated in a 37°C water bath for 1 hour and briefly vortexed every 10 minutes. Next, samples were passed through a 70μM filter and centrifuged at 2600 x g for 8 mins at 4 C, and the cell pellet was taken for antibody staining.

Blood samples were collected by submandibular bleed and red blood cells were depleted by magnetic-activated cell sorting (MACS) with anti-Ter-119 MicroBeads (Miltenyi Biotech, 130-049-901) following the manufacturer's protocol. Cells were pelleted and washed with HMI-9 media.

All samples, both blood and tissues, were stained with Zombie Aqua™ dye at 1:100 in PBS and washed with PBS following the manufacturer's protocol (BioLegend, 423101). Samples were then stained for 10 minutes at 4°C with a rabbit anti-AnTat1.1 polyclonal antibody diluted 1:15,000 in HMI-9 media and washed once with HMI-9 (antibody courtesy of Jay Bangs). Then, secondary antibody staining was performed for 10 minutes at 4°C with Anti-Rabbit IgG conjugated to Alexa Fluor® 488 fluorescent dye (Cell Signaling Technology, 4412S). Finally, samples were washed with cold PBS and resuspended in PBS for flow cytometry analysis. Samples were run on a Beckton Dickenson A3 Symphony flow cytometer and analysis was performed using FlowJo (version 10.6.1).

bioRxiv preprint doi: https://doi.org/10.1101/2022.06.27.497797; this version posted June 27, 2022. The copyright holder for this preprint (which was not certified by peer review) is the author/funder, who has granted bioRxiv a license to display the preprint in perpetuity. It is made available under aCC-BY-NC 4.0 International license.

Acknowledgments

We would like to kindly thank Jay Bangs for supplying us with the anti-AnTat1.1 antibody and Brice Rotureau for providing us with the chimeric triple reporter cell line. We thank Tricia Nilles and Worod Allak at the Becton Dickinson Immunology and Flow Cytometry core at Johns Hopkins Bloomberg School of Public Health for training, support, and technical assistance using the BD FACS Symphony A3. The facility is supported in part by CFAR: 5P30AI094189-04 (Chaisson). Data analysis was carried out at the Advanced Research Computing at Hopkins (ARCH) core facility (rockfish.jhu.edu), which is supported by the National Science Foundation (NSF) grant number OAC 1920103. AB was supported by NIH T32AI007417. NC was supported by NIH T32 OD011089. FR-F is supported by NIH NIGMS 1K99GM132557-01 and is an Investigator in the Chan Zuckerberg Biohub. MRM, AB, BB, and BZ were supported by Office of the Director, NIH (DP5OD023065).

References

1. WHO. Control and surveillance of human African trypanosomiasis: Report of a WHO Expert Committee. *WHO Tech Rep Ser*. 2013;(984):1-237. https://www.proquest.com/scholarly-journals/control-surveillance-human-african/docview/1504252667/se-2?accountid=11752.
2. Dumas M, Bouteille B, Buguet A. *Progress in Human African Trypanosomiasis, Sleeping Sickness*.; 2013. https://books.google.com/books?hl=en&lr=&id=zL_zBwAAQBAJ&oi=fnd&pg=PA1&ots=ni_8fjcZp-&sig=NfOo7lBHyt_z3EnRIk7S99tBCOk. Accessed April 29, 2022.
3. Crilly NP, Mugnier MR. Thinking outside the blood: Perspectives on tissue-resident Trypanosoma brucei. *PLOS Pathog*. 2021;17(9):e1009866. doi:10.1371/JOURNAL.PPAT.1009866
4. Kennedy PGE, Rodgers J. Clinical and neuropathogenetic aspects of human African trypanosomiasis. *Front Immunol*. 2019;10(JAN). doi:10.3389/fimmu.2019.00039
5. WHO. Trypanosomiasis, human African (sleeping sickness) Fact sheet. https://www.who.int/news-room/fact-sheets/detail/trypanosomiasis-human-african-(sleeping-sickness). Published 2022. Accessed April 29, 2022.
6. Magez S, Schwegmann A, Atkinson R, et al. The Role of B-cells and IgM Antibodies in Parasitemia, Anemia, and VSG Switching in Trypanosoma brucei–Infected Mice. Black S, ed. *PLoS Pathog*. 2008;4(8):e1000122. doi:10.1371/journal.ppat.1000122
7. Cross GAM, Kim H-S, Wickstead B. Capturing the variant surface glycoprotein repertoire (the VSGnome) of Trypanosoma brucei Lister 427. *Mol Biochem Parasitol*. 2014;195(1):59-73. doi:10.1016/j.molbiopara.2014.06.004
8. Hertz-Fowler C, Figueiredo LM, Quail MA, et al. Telomeric Expression Sites Are Highly Conserved in Trypanosoma brucei. Hall N, ed. *PLoS One*. 2008;3(10):e3527. doi:10.1371/journal.pone.0003527
9. Müller LSM, Cosentino RO, Förstner KU, et al. Genome organization and DNA accessibility control antigenic variation in trypanosomes. *Nature*. 2018;563(7729):121-125.
10. Cosentino R, Brink B, Siegel T. A phased genome assembly for allele-specific analysis in Trypanosoma brucei. *bioRxiv*. April 2021:2021.04.13.439624. doi:10.1101/2021.04.13.439624

bioRxiv preprint doi: https://doi.org/10.1101/2022.06.27.497797; this version posted June 27, 2022. The copyright holder for this preprint (which was not certified by peer review) is the author/funder, who has granted bioRxiv a license to display the preprint in perpetuity. It is made available under aCC-BY-NC 4.0 International license.

11. Kamper SM, Barbet AF. Surface epitope variation via mosaic gene formation is potential key to long-term survival of Trypanosoma brucei. *Mol Biochem Parasitol*. 1992;53(1-2):33-44. http://www.ncbi.nlm.nih.gov/entrez/query.fcgi?db=pubmed&cmd=Retrieve&dopt=AbstractPlus&list_uids=1380125.

12. Hall JPJ, Wang H, Barry JD. Mosaic VSGs and the scale of Trypanosoma brucei antigenic variation. Horn D, ed. *PLoS Pathog*. 2013;9(7):e1003502. http://www.ncbi.nlm.nih.gov/entrez/query.fcgi?db=pubmed&cmd=Retrieve&dopt=AbstractPlus&list_uids=23853603.

13. A case of sleeping sickness studied by precise enumerative methods: Regular periodical increase of the parasites disclosed. *Proc R Soc London Ser B, Contain Pap a Biol Character*. 1910;82(557):411-415. doi:10.1098/RSPB.1910.0035

14. Mugnier MR, Cross GAM, Papavasiliou FN. The in vivo dynamics of antigenic variation in Trypanosoma brucei. *Science (80-)*. 2015;347(6229):1470-1473. doi:10.1126/science.aaa4502

15. Jayaraman S, Harris C, Paxton E, et al. Application of long read sequencing to determine expressed antigen diversity in Trypanosoma brucei infections. Acosta-Serrano A, ed. *PLoS Negl Trop Dis*. 2019;13(4):e0007262. doi:10.1371/journal.pntd.0007262

16. Hall JPJ, Wang H, David Barry J. Mosaic VSGs and the Scale of Trypanosoma brucei Antigenic Variation. *PLoS Pathog*. 2013;9(7). doi:10.1371/JOURNAL.PPAT.1003502

17. Capewell P, Cren-Travaillé C, Marchesi F, et al. The skin is a significant but overlooked anatomical reservoir for vector-borne African trypanosomes . *Elife*. 2016;5:157. https://elifesciences.org/articles/17716.

18. Camara M, Soumah AM, Ilboudo H, et al. Extravascular Dermal Trypanosomes in Suspected and Confirmed Cases of gambiense Human African Trypanosomiasis. *Clin Infect Dis*. 2021;73(1):12-20. doi:10.1093/cid/ciaa897

19. De Niz M, Brás D, Ouarné M, et al. Organotypic endothelial adhesion molecules are key for Trypanosoma brucei tropism and virulence. *Cell Rep*. 2021;36(12):109741. doi:10.1016/J.CELREP.2021.109741

20. Trindade S, Rijo-Ferreira F, Carvalho T, et al. Trypanosoma brucei Parasites Occupy and Functionally Adapt to the Adipose Tissue in Mice. *Cell Host Microbe*. 2016;19(6):837-848. doi:10.1016/j.chom.2016.05.002

21. Carvalho T, Trindade S, Pimenta S, Santos AB, Rijo-Ferreira F, Figueiredo LM. Trypanosoma brucei triggers a marked immune response in male reproductive organs. *PLoS Negl Trop Dis*. 2018;12(8). doi:10.1371/journal.pntd.0006690

22. Quintana JF, Chandrasegaran P, Sinton MC, et al. Integrative single cell and spatial transcriptomic analysis reveal reciprocal microglia-plasma cell crosstalk in the mouse brain during chronic Trypanosoma brucei infection. *bioRxiv*. March 2022:2022.03.25.485502. doi:10.1101/2022.03.25.485502

23. Reuter C, Imdahl F, Hauf L, et al. Vector-borne Trypanosoma brucei parasites develop in artificial human skin and persist as skin tissue forms. *bioRxiv*. May 2021:2021.05.13.443986. doi:10.1101/2021.05.13.443986

24. Salanti A, Dahlbäck M, Turner L, et al. Evidence for the Involvement of VAR2CSA in Pregnancy-associated Malaria. *J Exp Med*. 2004;200(9):1197-1203. doi:10.1084/JEM.20041579

bioRxiv preprint doi: https://doi.org/10.1101/2022.06.27.497797; this version posted June 27, 2022. The copyright holder for this preprint (which was not certified by peer review) is the author/funder, who has granted bioRxiv a license to display the preprint in perpetuity. It is made available under aCC-BY-NC 4.0 International license.

25. Duffy PE, Fried M. Plasmodium falciparum adhesion in the placenta. *Curr Opin Microbiol*. 2003;6(4):371-376. doi:10.1016/S1369-5274(03)00090-0

26. Jonsson A -B, Ilver D, Falk P, Pepose J, Normark S. Sequence changes in the pilus subunit lead to tropism variation of Neisseria gonorrhoeae to human tissue. *Mol Microbiol*. 1994;13(3):403-416. doi:10.1111/J.1365-2958.1994.TB00435.X

27. Silva Pereira S, Jackson AP, Figueiredo LM. Evolution of the variant surface glycoprotein family in African trypanosomes. *Trends Parasitol*. 2022;38(1):23-36. doi:10.1016/J.PT.2021.07.012

28. Wiedemar N, Graf FE, Zwyer M, et al. Beyond immune escape: a variant surface glycoprotein causes suramin resistance in Trypanosoma brucei. *Mol Microbiol*. 2018;107(1):57-67. doi:10.1111/MMI.13854

29. Liu D, Albergante L, Newman TJ, Horn D. Faster growth with shorter antigens can explain a VSG hierarchy during African trypanosome infections: a feint attack by parasites. *Sci Rep*. 2018;8(1):10922. doi:10.1038/s41598-018-29296-8

30. Engstler M, Boshart M. Cold shock and regulation of surface protein trafficking convey sensitization to inducers of stage differentiation in Trypanosoma brucei. *Genes Dev*. 2004;18(22):2798. doi:10.1101/GAD.323404

31. Calvo-Alvarez E, Cren-Travaillé C, Crouzols A, Rotureau B. A new chimeric triple reporter fusion protein as a tool for in vitro and in vivo multimodal imaging to monitor the development of African trypanosomes and Leishmania parasites. *Infect Genet Evol*. 2018;63:391-403. doi:10.1016/J.MEEGID.2018.01.011

32. Morrison LJ, Majiwa P, Read AF, Barry JD. Probabilistic order in antigenic variation of Trypanosoma brucei. *Int J Parasitol*. 2005;35(9):961-972. http://www.ncbi.nlm.nih.gov/entrez/query.fcgi?db=pubmed&cmd=Retrieve&dopt=AbstractPlus&list_uids=16000200.

33. Zeelen J, Straaten M van, Verdi J, et al. Structure of Trypanosome Coat Protein VSGsur and Function in Suramin Resistance. *Nat Microbiol*. 2021;6(3):392. doi:10.1038/S41564-020-00844-1

34. So J, Sudlow S, Sayeed A, et al. Trypanosomal variant surface glycoprotein expression in human African trypanosomiasis patients. *bioRxiv*. September 2021:2021.09.09.459620. doi:10.1101/2021.09.09.459620

35. Cadavid D, Pennington PM, Kerentseva TA, Bergström S, Barbour AG. Immunologic and genetic analyses of VmpA of a neurotropic strain of Borrelia turicatae. *Infect Immun*. 1997;65(8):3352. doi:10.1128/IAI.65.8.3352-3360.1997

36. Caljon G, van Reet N, De Trez C, Vermeersch M, Pérez-Morga D, Van Den Abbeele J. The Dermis as a Delivery Site of Trypanosoma brucei for Tsetse Flies. Peters NC, ed. *PLoS Pathog*. 2016;12(7):e1005744. http://dx.plos.org/10.1371/journal.ppat.1005744.

37. Morrison L, Majiwa P, Read A, for JB-I journal, 2005 undefined. Probabilistic order in antigenic variation of Trypanosoma brucei. *Elsevier*. https://www.sciencedirect.com/science/article/pii/S0020751905001712. Accessed April 29, 2022.

38. Glover L, Alsford S, Horn D. DNA Break Site at Fragile Subtelomeres Determines Probability and Mechanism of Antigenic Variation in African Trypanosomes. *PLoS Pathog*. 2013;9(3):1003260. doi:10.1371/journal.ppat.1003260

39. Boothroyd CE, Dreesen O, Leonova T, et al. A yeast-endonuclease-generated DNA

bioRxiv preprint doi: https://doi.org/10.1101/2022.06.27.497797; this version posted June 27, 2022. The copyright holder for this preprint (which was not certified by peer review) is the author/funder, who has granted bioRxiv a license to display the preprint in perpetuity. It is made available under aCC-BY-NC 4.0 International license.

546 break induces antigenic switching in Trypanosoma brucei. *Nature*. 2009;459(7244):278-
547 281. doi:10.1038/nature07982

548 40. Magez S, Schwegmann A, Atkinson R, et al. The role of B-cells and IgM antibodies in
549 parasitemia, anemia, and VSG switching in Trypanosoma brucei-infected mice. *PLoS*
550 *Pathog*. 2008;4(8):e1000122.
551 http://www.ncbi.nlm.nih.gov/entrez/query.fcgi?db=pubmed&cmd=Retrieve&dopt=Abstract
552 Plus&list_uids=18688274.

553 41. Schopf LR, Filutowicz H, Bi X-J, Mansfiled JM. Trypanosome Variant Surface
554 Glycoprotein Antigen-Specific Th1-Cell Response to the Isotype Switch in the Presence
555 of a Polarized Interleukin-4-Dependent Immunoglobulin G1. *Infect Immun*.
556 1998;66(2):451. http://iai.asm.org/content/66/2/451http://iai.asm.org/content/66/2/451#ref-
557 list-1. Accessed January 4, 2019.

558 42. Hector RF, Collins MS, Pennington JE. Treatment of Experimental Pseudomonas
559 aeruginosa Pneumonia with a Human IgM Monoclonal Antibody. *J Infect Dis*.
560 1989;160(3):483-489. doi:10.1093/INFDIS/160.3.483

561 43. BARTH WF, WOCHNER RD, WALDMANN TA, FAHEY JL. Metabolism of Human
562 Gamma Macroglobulins. *J Clin Invest*. 1964;43(6):1036. doi:10.1172/JCI104987

563 44. Fu L, Niu B, Zhu Z, Wu S, Li W. CD-HIT: accelerated for clustering the next-generation
564 sequencing data. *Bioinformatics*. 2012;28(23):3150.
565 doi:10.1093/BIOINFORMATICS/BTS565

566
567
568
569
570
571
572
573
574
575
576
577
578
579

bioRxiv preprint doi: https://doi.org/10.1101/2022.06.27.497797; this version posted June 27, 2022. The copyright holder for this preprint (which was not certified by peer review) is the author/funder, who has granted bioRxiv a license to display the preprint in perpetuity. It is made available under aCC-BY-NC 4.0 International license.

580 **Supplemental Figures**

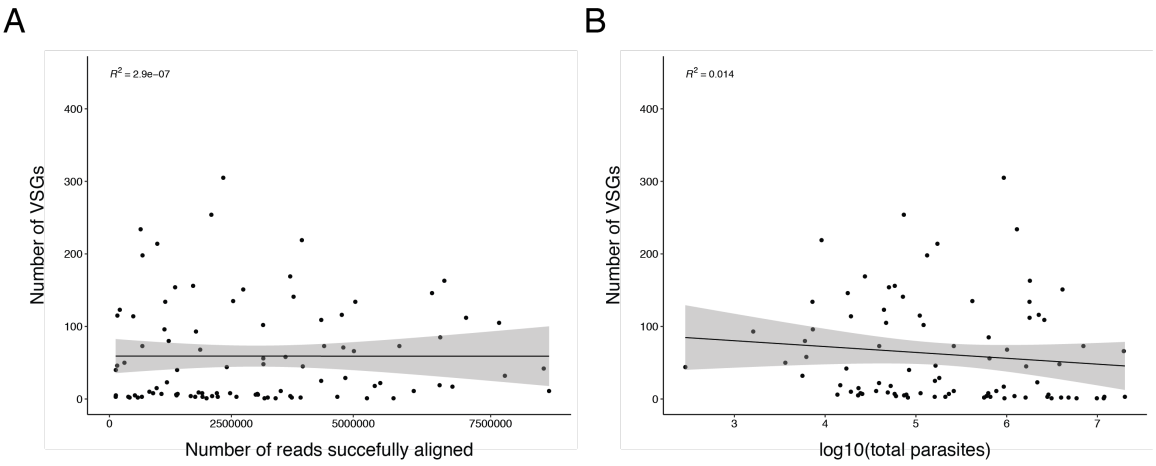

Supplemental Figure 1: VSG diversity counts are not biased by the sample's read count or parasite count. (A) A comparison of the number of reads successfully aligned in a sample and the number of VSGs found. **(B)** A comparison of the total number of parasites and the number of VSGs found in each sample.

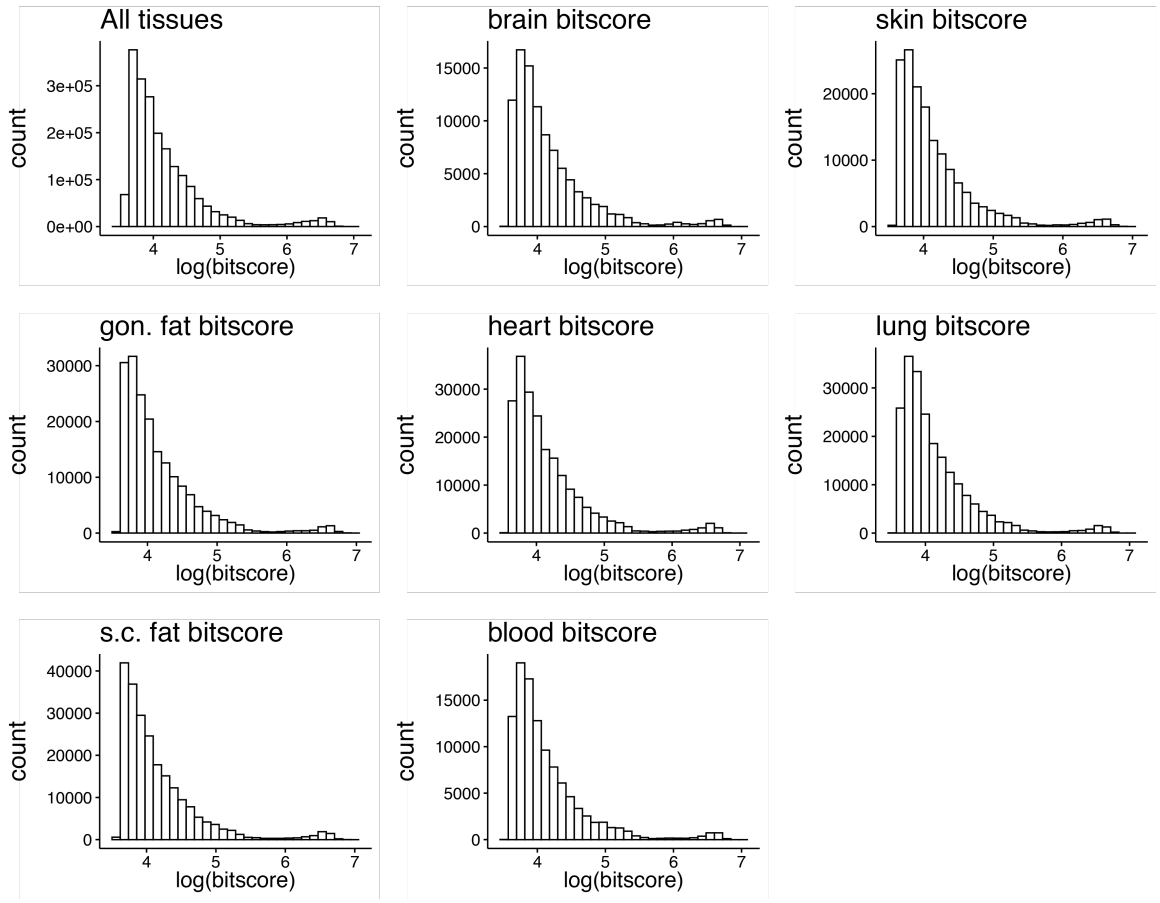

Supplemental Figure 2: No tissue-specific VSGs or VSG sequence motifs exist. Distribution of bitscores across tissue compartments. The similarity of VSGs extracted from each tissue as measured by bitscore, a sequence similarity metric normalized to the database size, allows for comparing tissue compartments with different numbers of total VSGs expressed in each tissue. No statistical significance was found.

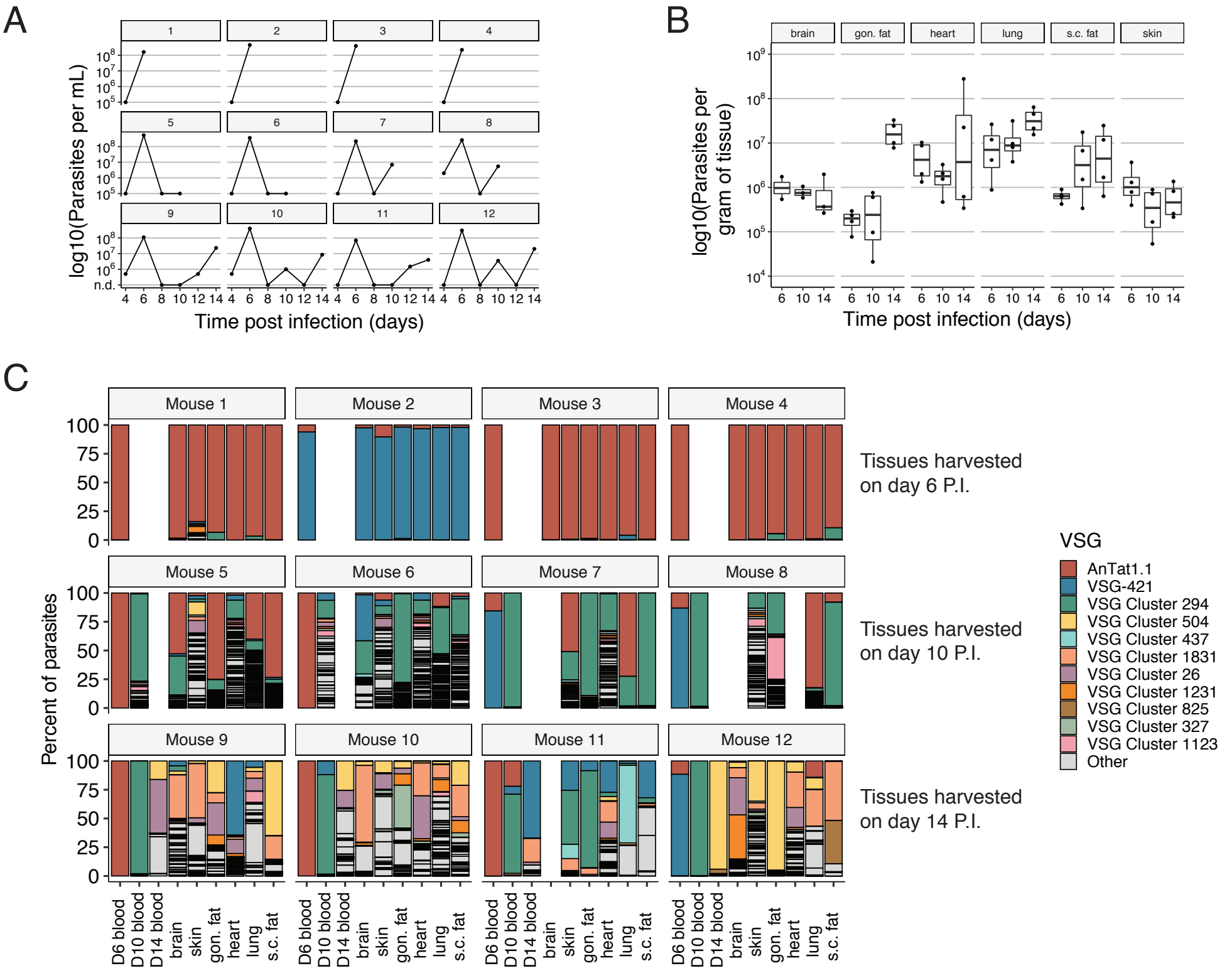
A
1
2
3
4
5
6
7
8
9
10
11
12
log10(Parasites per mL)
n.d.
Time post infection (days)
B
brain
gon. fat
heart
lung
s.c. fat
skin
log10(Parasites per gram of tissue)
Time post infection (days)
C
Mouse 1
Mouse 2
Mouse 3
Mouse 4
Mouse 5
Mouse 6
Mouse 7
Mouse 8
Mouse 9
Mouse 10
Mouse 11
Mouse 12
Percent of parasites
Tissues harvested on day 6 P.I.
Tissues harvested on day 10 P.I.
Tissues harvested on day 14 P.I.
D6 blood
D10 blood
D14 blood
brain
skin
gon. fat
heart
lung
s.c. fat
VSG
AnTat1.1
VSG-421
VSG Cluster 294
VSG Cluster 504
VSG Cluster 437
VSG Cluster 1831
VSG Cluster 26
VSG Cluster 1231
VSG Cluster 825
VSG Cluster 327
VSG Cluster 1123
Other

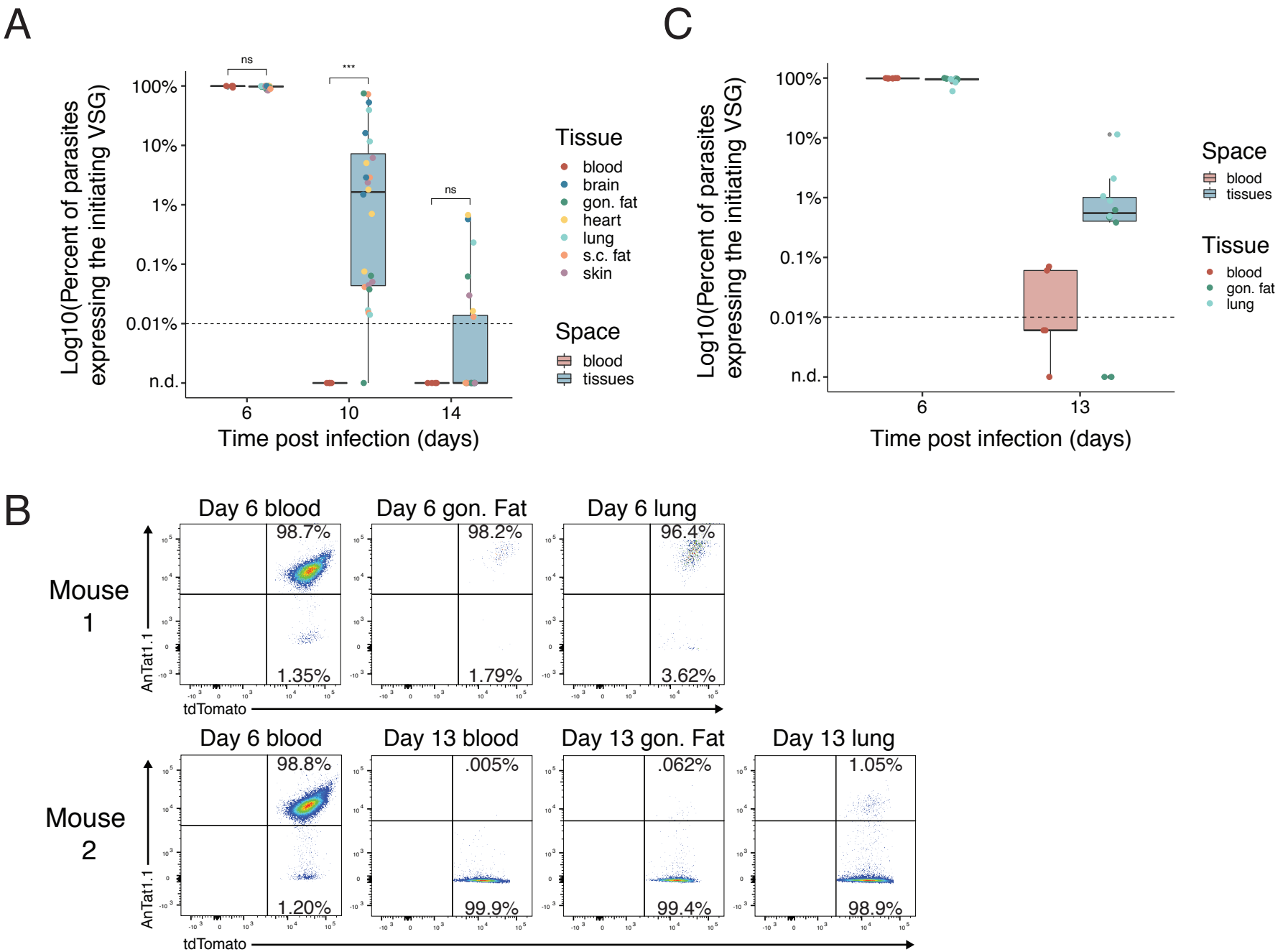
A
ns
***
ns
100%
10%
1%
0.1%
0.01%
n.d.
Log10(Percent of parasites expressing the initiating VSG)
6
10
14
Time post infection (days)
Tissue
blood
brain
gon. fat
heart
lung
s.c. fat
skin
Space
blood
tissues
C
100%
10%
1%
0.1%
0.01%
n.d.
Log10(Percent of parasites expressing the initiating VSG)
6
13
Time post infection (days)
Space
blood
tissues
Tissue
blood
gon. fat
lung
B
Mouse 1
Day 6 blood
Day 6 gon. Fat
Day 6 lung
98.7%
1.35%
98.2%
1.79%
96.4%
3.62%
AnTat1.1
tdTomato
Mouse 2
Day 6 blood
Day 13 blood
Day 13 gon. Fat
Day 13 lung
98.8%
1.20%
.005%
99.9%
.062%
99.4%
1.05%
98.9%
AnTat1.1
tdTomato

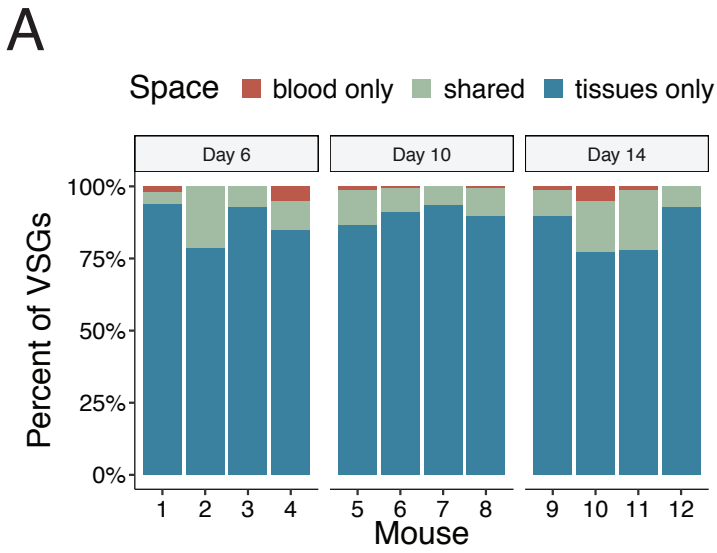
A
Space
blood only
shared
tissues only
Day 6
Day 10
Day 14
Percent of VSGs
100%
75%
50%
25%
0%
1
2
3
4
5
6
7
8
9
10
11
12
Mouse

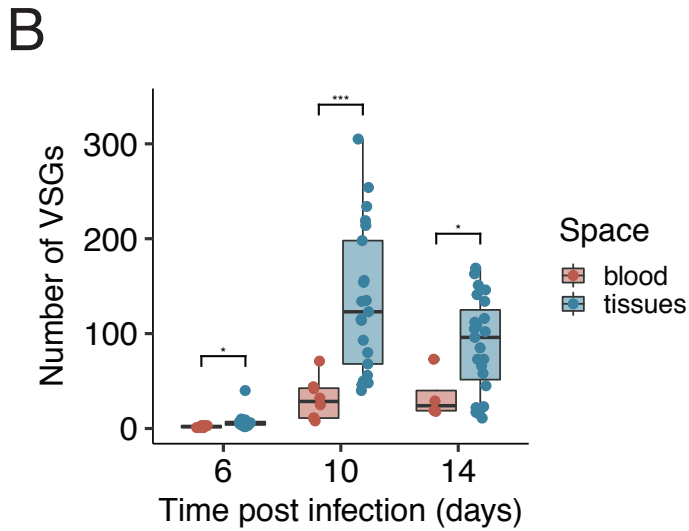
B
Number of VSGs
300
200
100
0
***
*
*
6
10
14
Time post infection (days)
Space
blood
tissues

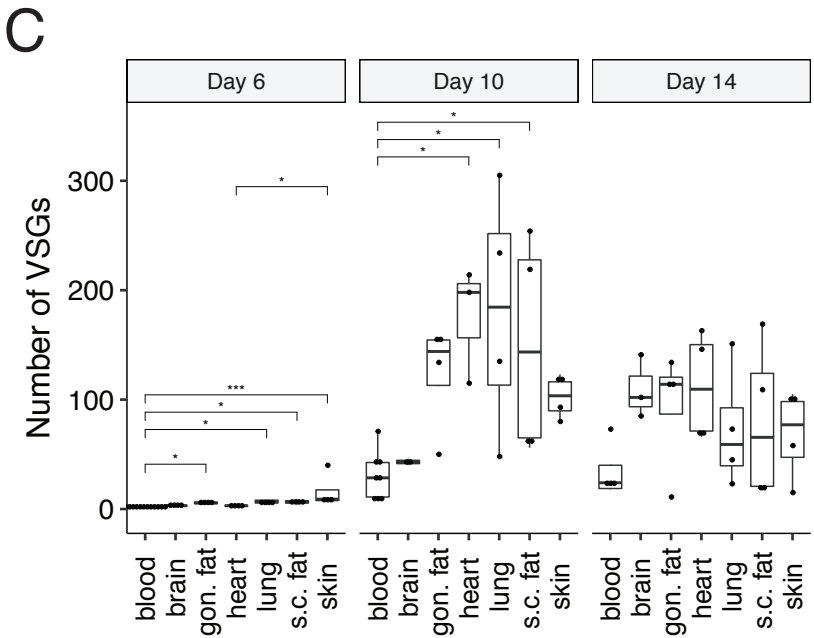
C
Day 6
Day 10
Day 14
Number of VSGs
300
200
100
0
blood
brain
gon. fat
heart
lung
s.c. fat
skin

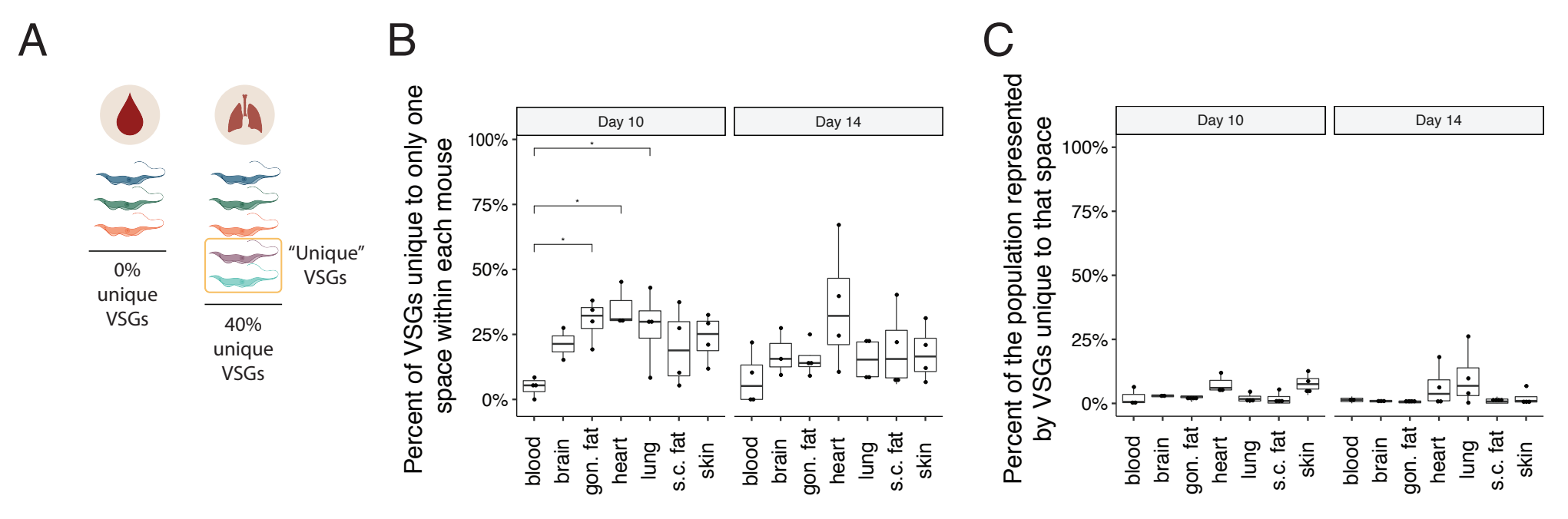
A
0%
unique
VSGs
"Unique"
VSGs
40%
unique
VSGs
B
Percent of VSGs unique to only one space within each mouse
Day 10
Day 14
100%
75%
50%
25%
0%
blood
brain
gon. fat
heart
lung
s.c. fat
skin
C
Percent of the population represented by VSGs unique to that space
Day 10
Day 14
100%
75%
50%
25%
0%
blood
brain
gon. fat
heart
lung
s.c. fat
skin

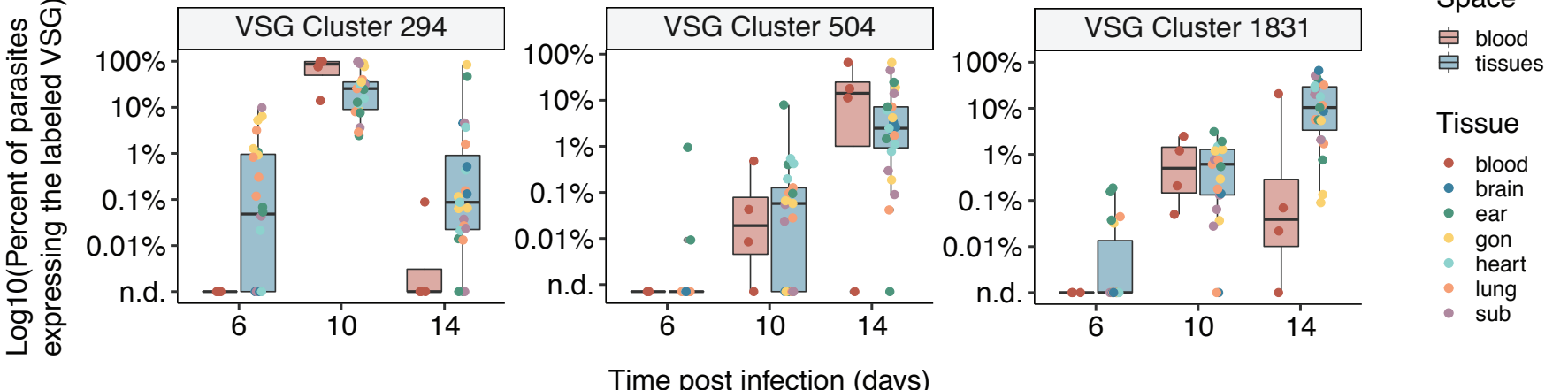
VSG Cluster 294
VSG Cluster 504
VSG Cluster 1831
Log10(Percent of parasites expressing the labeled VSG)
100%
10%
1%
0.1%
0.01%
n.d.
6
10
14
Time post infection (days)
Space
blood
tissues
Tissue
blood
brain
ear
gon
heart
lung
sub

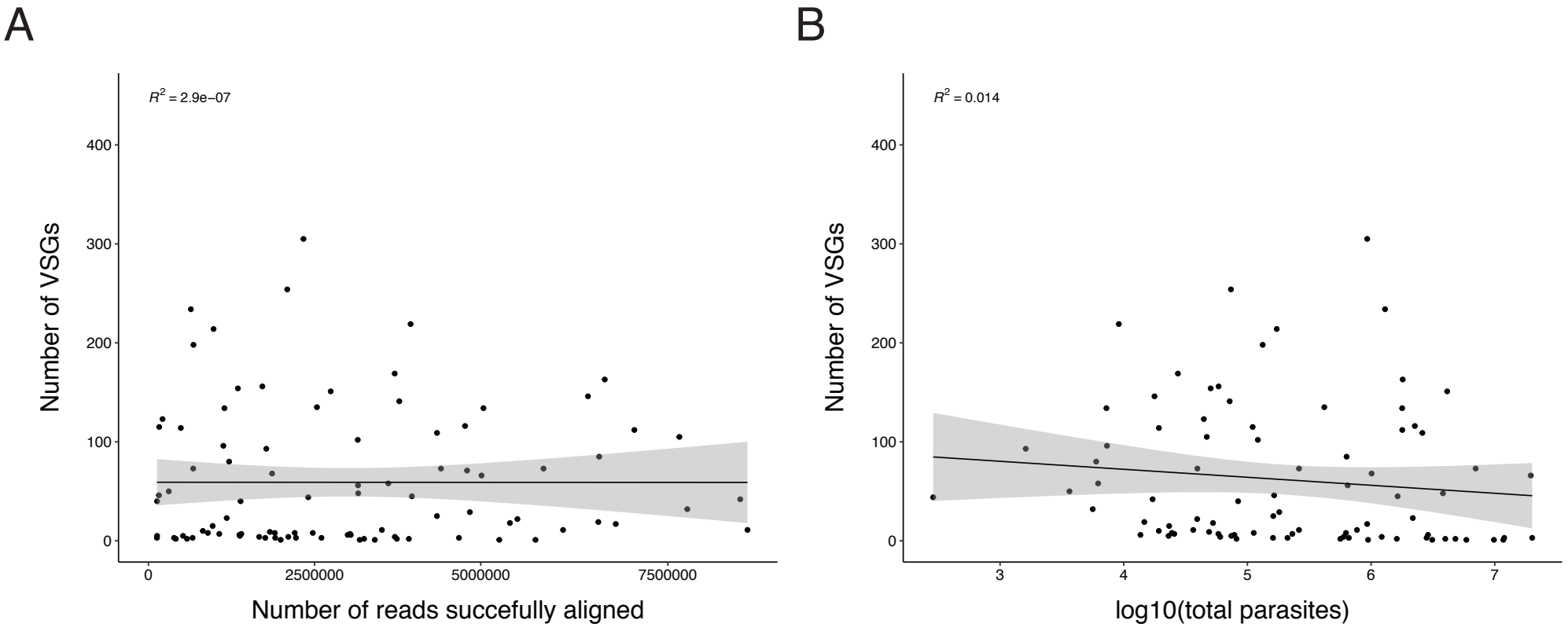
A
R^2 = 2.9e−07
Number of VSGs
400
300
200
100
0
0
2500000
5000000
7500000
Number of reads succefully aligned
B
R^2 = 0.014
Number of VSGs
400
300
200
100
0
3
4
5
6
7
log10(total parasites)

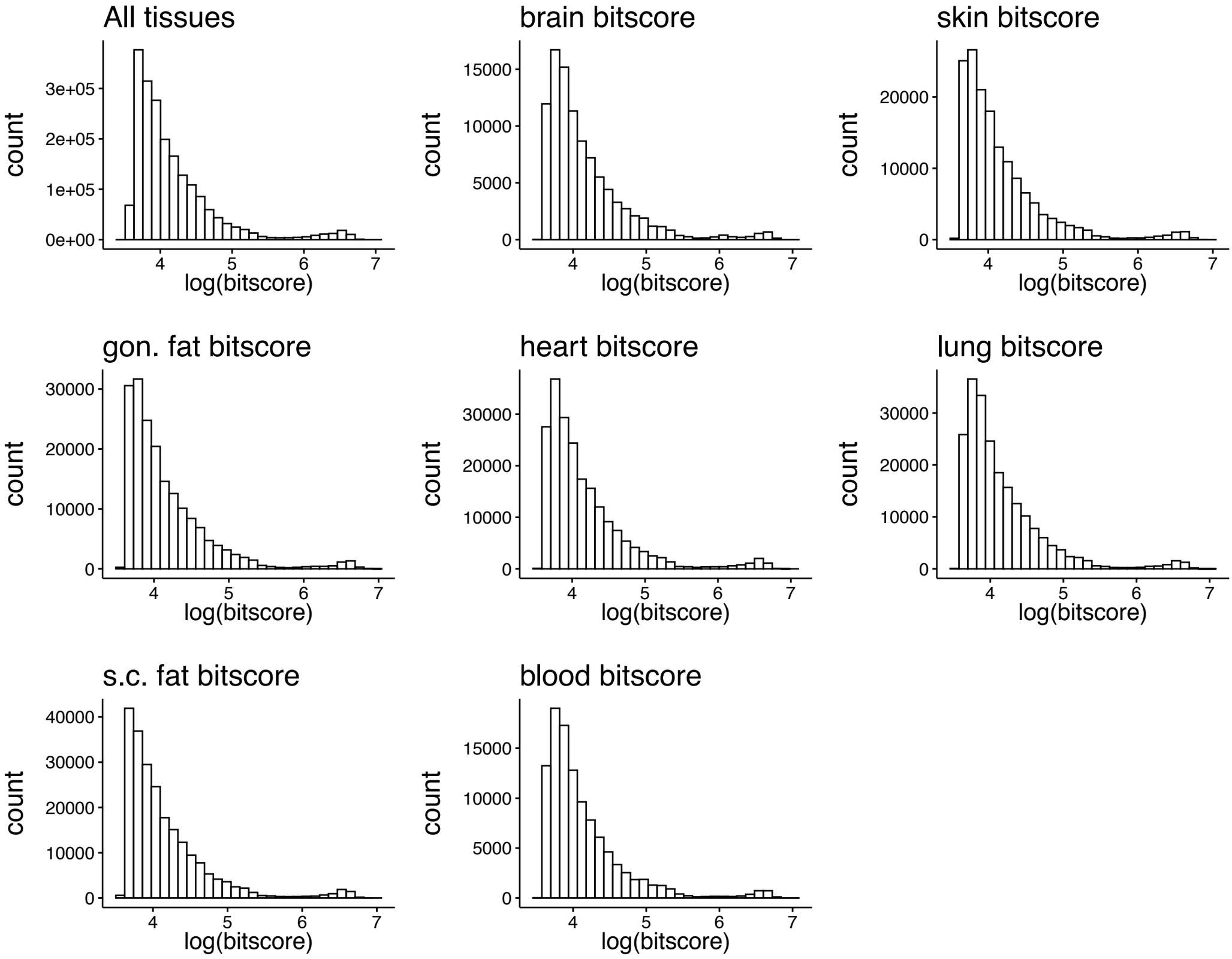
All tissues
brain bitscore
skin bitscore
gon. fat bitscore
heart bitscore
lung bitscore
s.c. fat bitscore
blood bitscore
count
log(bitscore)
0e+00
1e+05
2e+05
3e+05
0
5000
10000
15000
20000
30000
40000
4
5
6
7